ELSEVIER

Experimental Thermal and Fluid Science 24 (2001) 47–59

Experimental Thermal and Fluid Science

www.elsevier.nl/locate/etfs

Chebyshev spectral method and Chebyshev noise processing procedure for vorticity calculation in PIV post-processing

Suchuan Dong, Hui Meng *

Department of Mechanical & Aerospace Engineering, State University of New York – SUNY, 324 Jarvis Hall, Buffalo, Buffalo, NY 14260-4400, USA

Received 13 March 2000; accepted 2 October 2000

Abstract

Chebyshev spectral method and Chebyshev noise processing procedure are proposed for the calculation of vorticity from PIV experimental data. The Chebyshev spectral method offers superior intrinsic accuracy of derivative calculations. To overcome its noise sensitivity, the Chebyshev noise processing procedure can be applied prior to the derivative calculation to remove the high-frequency noise in the Chebyshev transform space. We compare the Chebyshev spectral method against the least-squares approach and test their performance in the calculation of vorticity with an Oseen vortex and with PIV data of the wake of a trapezoidal mixing tab. It is found that for clean velocity data the Chebyshev spectral method is extremely accurate. However, the Chebyshev spectral method alone is found to be more sensitive to noise than the least-squares method. When the Chebyshev noise processing procedure is applied together with the Chebyshev spectral method it greatly reduces the error and makes the Chebyshev spectral method more accurate than the least-squares method for a wide range of vorticity values. A special requirement imposed by the Chebyshev spectral method is that the PIV velocity processing must be carried out on special grids such as Gauss–Lobatto points.

Keywords: Spectral methods; Vorticity; PIV

1. Introduction

Particle image velocimetry (PIV) provides instantaneous velocity data of a flow in a 2D plane (or in a 3D volume with the newly emerged holographic PIV [1–3]). A great deal of information can be obtained about the flow if the vorticity of the flow field can be accurately computed from the PIV (including holographic PIV) measurements. Vorticity calculation methods are usually based on a numerical derivative calculation. Besides vorticity, evaluation of the strain rate tensor also requires calculating the derivatives of the velocity field. Many benefits can be obtained from accurate derivative calculations. For example, various vortex identification methods based on eigenvalues or invariants of the strain rate tensor [4,5] can be implemented on PIV measurements. Unfortunately experimental noise and spuriously deleted vectors in PIV data pose great challenges to the reliability of velocity derivatives and thus the vorticity. An ideal vorticity calculation method should be accurate as well as insensitive to noise. Hence, accuracy and noise sensitivity are two aspects one has to consider when devising vorticity calculation methods in post-processing of PIV data.

Existing derivative calculation methods include finite difference, least-squares approach, Richardson's extrapolation, and various polynomial fittings. The finite difference schemes are the most basic methods for calculating derivatives. The intrinsic accuracy of the finite difference schemes increases with the order of the scheme. Lele [6] proposed compact finite difference schemes of up to tenth order for first and second derivatives. Mahesh [7] gave a high-order finite difference scheme in which the first- and second-order derivatives are computed simultaneously rather than separately. However, despite the increased accuracy, the noise sensitivity usually also increases with the order of the scheme. Abrahamson and Lonnes [8] proposed a least-squares approach, in which the planar velocity field is approximated with a linear combination of a uniform velocity, a line vortex, a line source and a shear layer. Although the intrinsic accuracy of the least-squares method is similar to that of the second-order finite

* Corresponding author. Tel.: +1-716-645-2593 ext. 2354; fax: +1-716-645-3875.

E-mail address: huimeng@eng.buffalo.edu (H. Meng).

0894-1777/01/$ - see front matter
PII: S0894-1777(00)00057-1

Nomenclature

A	area, m^2
C	Chebyshev transform matrix, dimensionless
E	error, dimensionless
D	derivative matrix in Chebyshev spectral method, dimensionless
K	error transfer coefficient, dimensionless
L	length, m
M	mode number
N	number of grid points, dimensionless
RMS	root-mean-square error of vorticity, s^{-1}
T	Chebyshev polynomial, dimensionless
U	velocity component in x direction, m/s
V	velocity component in y direction, m/s
c	multiplication coefficient in Chebyshev transform, dimensionless
$\bar{c}$	multiplication coefficient in Chebyshev transform, dimensionless
f	a generic function, dimensionless
$\hat{f}$	Chebyshev coefficient of function f, dimensionless
$\hat{f}^{(q)}$	Chebyshev coefficient of $d^q f/dx^q$, dimensionless
i, j, k, m, n	indices, dimensionless
r	radial coordinate in cylindrical system, m
t	time, s
u	velocity component in x direction, m/s
v	velocity component in y direction, m/s
w	coefficient in Chebyshev spectral method, dimensionless
x	coordinate of Cartesian system, m
y	coordinate of Cartesian system, m
z	coordinate in cylindrical system, m

Greek symbols

Γ	circulation, m^2/s
Δ	measurement error, dimensionless
ψ_{cut}	energy ratio
θ	angular coordinate in cylindrical system, dimensionless
γ	coefficient in Chebyshev spectral method, dimensionless
ω	vorticity, s^{-1}
ω_{comp}	computed vorticity, s^{-1}
ω_{ex}	exact vorticity, s^{-1}
η	similarity variable in the Oseen vortex, dimensionless
δ	parameter in the Oseen vortex, m
ξ	random variable, dimensionless
ε	relative error of vorticity calculation, dimensionless

Subscripts and superscripts

comp	computed
ex	exact
$\hat{}$	in Chebyshev transform space
$\bar{}$	exact quantity
q	order of derivative

difference, the method is very robust and far less sensitive to experimental noise because of the least-squares minimization requirement. Hence, the least-squares approach is a more suitable derivative-calculation method for PIV experimental data. In the same work [8], Abrahamson and Lonnes also discussed the circulation method for vorticity calculation. Using Richardson's extrapolation principle Lourenco and Krothapalli [9] suggested an adaptive scheme to compute the vorticity aiming at minimizing the total error affecting the vorticity estimation. Lecuona et al. [10] suggested an algorithm in which the derivatives are approximated with a linear combination of the velocity data. Fouras and Soria [11] proposed to approximate the local velocity in terms of a set of base functions and minimize the Chi-square of the difference between the real velocity and the approximated velocity; then the vorticity can be obtained analytically. The intrinsic accuracy of all the above methods is generally limited by the orders of the schemes, but higher orders are usually associated with higher noise sensitivity. In order to improve the reliability of the calculation of vorticity from PIV experimental data, it is desirable to explore more accurate representations of velocity derivatives, for example, through the use of spectral methods.

Spectral methods are widely used in direct numerical simulations (DNS) of fluid flows due to the high accuracy of spectral representations of derivatives. Since in PIV experiments we usually encounter non-periodic flow domains, which are better approximated by the Chebyshev polynomials than by the Fourier series, we investigate the Chebyshev spectral method for calculating the vorticity from PIV experimental data in this paper. In spectral methods the velocity field is expanded in terms of some global function and represented uniquely by a truncated series of the expansion coefficients. The derivatives of the velocity field are first computed with the expansion coefficients in the transform space and then the physical space solutions are obtained with an inverse transformation.

Since in spectral methods the derivative at any point is calculated using the velocity information on all the points from the same row and the same column, the experimental noise may potentially affect spectral methods more significantly than low-order schemes. To overcome the problem we propose the Chebyshev noise processing procedure (CNPP), which removes high-frequency noise modes but retains the physical modes in the Chebyshev transform space. The CNPP can be applied in conjunction with the Chebyshev spectral method to improve the accuracy of the derivatives in the presence of noise.

In Section 2 the general idea of derivative calculation with the Chebyshev spectral method is presented. We analyze the error transfer of the Chebyshev spectral method and formulate the Chebyshev noise processing

procedure in Section 3. After that we conduct a comparison between the Chebyshev spectral method in conjunction with the Chebyshev noise processing procedure and the least-squares method. The comparison is carried out with the Oseen vortex and with PIV experimental velocity data in the wake of a mixing tab.

2. Chebyshev spectral method for derivative calculation

In this section we give a brief introduction to the transforms used in the Chebyshev spectral method. Detailed investigation of various aspects of spectral methods can be found in Cannuto et al. [12] and Hussaini and Zang [13].

The Chebyshev polynomial

$$T_k(x) = \cos(k\cos^{-1}x) \tag{1}$$

is widely used in numerical approximations of non-periodic problems. The discrete Chebyshev transform requires special distributions of the grid points in the form of, for example, Chebyshev–Gauss points, Chebyshev–Gauss–Radau points or Chebyshev–Gauss–Lobatto points [12]. The most commonly used distribution, which is considered in this paper, is Gauss–Lobatto grid points given by:

$$x_j = \cos\frac{\pi j}{N}, \quad j = 0,\ldots,N, \tag{2}$$

where $(N+1)$ is the total number of grid points. Then the discrete Chebyshev transform can be expressed as

$$\hat{f}_k = \sum_{j=0}^{N} C_{kj} f(x_j), \quad k = 0,\ldots,N, \tag{3}$$

where $f(x_j)$ is a function defined on the Gauss–Lobatto points, $\hat{f}_k$ are the Chebyshev coefficients of the function, and

$$C_{kj} = \frac{2}{N\bar{c}_j\bar{c}_k}\cos\frac{\pi jk}{N}, \tag{4}$$

$$\bar{c}_j = \begin{cases} 2 & j = 0, N, \\ 1 & \text{otherwise.} \end{cases} \tag{5}$$

The inverse Chebyshev transform is given by

$$f(x_j) = \sum_{k=0}^{N} (C^{-1})_{jk}\hat{f}_k, \tag{6}$$

where

$$(C^{-1})_{jk} = \cos\frac{\pi jk}{N} = T_k(x_j). \tag{7}$$

The Chebyshev coefficients of $\mathrm{d}f/\mathrm{d}x$ are related to those of f according to equation

$$2k\hat{f}_k = c_{k-1}\hat{f}^{(1)}_{k-1} - \hat{f}^{(1)}_{k+1}, \quad k \geqslant 1, \tag{8}$$

where $\hat{f}^{(1)}_k$ are the Chebyshev coefficients of $\mathrm{d}f/\mathrm{d}x$, and $c_k = 2$ if $k = 0$, or 1 if $k \geqslant 1$. Note that $\hat{f}^{(1)}_k = 0$ for $k \geqslant N$. The coefficient $\hat{f}^{(1)}_k$ can be computed with the following recurrence relation in decreasing order:

$$c_k\hat{f}^{(1)}_k = \hat{f}^{(1)}_{k+2} + 2(k+1)\hat{f}_{k+1}, \quad 0 \leqslant k \leqslant N-1. \tag{9}$$

The relation is generalized to higher order as

$$c_k\hat{f}^{(q)}_k = \hat{f}^{(q)}_{k+2} + 2(k+1)\hat{f}^{(q-1)}_{k+1}, \tag{10}$$

where $\hat{f}^{(q)}_k$ are the Chebyshev coefficients of $\mathrm{d}^q f/\mathrm{d}x^q$. This relation can be used to compute high-order derivatives. Compared with second-order finite difference method, which estimates the derivative from a parabola that interpolates the function at the point of interest and two adjacent grid points (for central finite difference), the spectral approximation takes advantage of all the information about the function. While the finite difference method produces a second-order accurate derivative with the error decreasing as $1/N^2$ (N being the number of grid points), the error from the global method decreases exponentially [13].

One requirement of applying the Chebyshev spectral method for processing experimental data is the special grid point distribution. PIV experimental velocity data are usually obtained on equally spaced grid points, but the Chebyshev spectral method requires that the velocity data be computed directly on the Gauss–Lobatto grid points during PIV data processing. This would be straightforward if the PIV raw image of the flow field is partitioned such that the centers of the interrogation cells have the Gauss–Lobatto data point distribution.

Similar to its applications in numerical simulations, the Chebyshev spectral method proposed here for the purpose of vorticity calculation is suitable only for those simplified geometries that can accommodate the special grid requirements. It is particularly relevant to wall-bounded flows because more grid points are located in the regions of strongest gradients near the wall. However, this technique may not be directly used for generalized geometries such as around turbine blades and pipe bends or in situations where extensive maskings of images are required. This method may also become unfavorable for free shear flows, where the strongest gradients are located in the middle of the domain.

3. Error transfer analysis and Chebyshev noise processing procedure

3.1. Error transfer analysis

Consider the 2D velocity data (u, v) obtained by PIV measurements on Gauss–Lobatto grid points defined by Eq. (2) in a 2D plane (x, y). We would like to evaluate the relationship between the error in the velocity data and the error in the vorticity computed with Chebyshev spectral method. For this purpose it is more convenient to employ another form of the Chebyshev spectral method for derivative calculation. The derivative calculation procedure outlined in Section 2 can be reduced to the following relation in physical space:

$$\left.\frac{\mathrm{d}f}{\mathrm{d}x}\right|_{x_i} = \sum_{i=0}^{N} D_{i,j}^{N} f(x_j), \tag{11}$$

where the matrix $D_{i,j}^{N}$ is given by

$$D_{i,j}^{N} = \begin{cases} \frac{\bar{c}_i}{\bar{c}_j}\frac{(-1)^{i+j}}{x_i - x_j}, & i \neq j, \\ \frac{-x_j}{2(1-x_j^2)}, & 1 \leqslant i = j \leqslant N-1, \\ \frac{2N^2+1}{6}, & i = j = 0, \\ -\frac{2N^2+1}{6}, & i = j = N. \end{cases} \tag{12}$$

According to the definition of out-of-plane vorticity

$$\omega(x,y) = \frac{\partial v}{\partial x} - \frac{\partial u}{\partial y}, \tag{13}$$

we have, with the Chebyshev spectral method,

$$\omega(x_i,y_j) = \sum_{m=0}^{N_x} D_{i,m}^{N_x} v(x_m,y_j) - \sum_{n=0}^{N_y} D_{j,n}^{N_y} u(x_i,y_n), \tag{14}$$

where (N_x+1) and (N_y+1) are the number of grid points in x and y directions, respectively.

Let us assume that

$$u(x_i,y_j) = \bar{u}(x_i,y_j) \pm \Delta u(x_i,y_j), \tag{15}$$

$$v(x_i,y_j) = \bar{v}(x_i,y_j) \pm \Delta v(x_i,y_j), \tag{16}$$

where $\bar{u}(x_i,y_j)$ is the exact velocity value at point (x_i,y_j) and $\Delta u(x_i,y_j)$ is the measurement error. Further, the computed vorticity can be written as

$$\omega(x_i,y_j) = \bar{\omega}(x_i,y_j) \pm \Delta\omega(x_i,y_j), \tag{17}$$

where the error of vorticity is estimated from Eq. (14) based on uncertainty theory:

$$\Delta\omega(x_i,y_j) = \sum_{m=0}^{N_x} \left|D_{i,m}^{N_x}\right| \Delta v(x_m,y_j) + \sum_{n=0}^{N_y} \left|D_{j,n}^{N_y}\right| \Delta u(x_i,y_n). \tag{18}$$

The relative error of the vorticity is expressed by

$$\frac{\Delta\omega(x_i,y_j)}{|\bar{\omega}(x_i,y_j)|} = \sum_{m=0}^{N_x} K_{ij,m}^{v} \frac{\Delta v(x_m,y_j)}{|\bar{v}(x_m,y_j)|} + \sum_{n=0}^{N_y} K_{ij,n}^{u} \frac{\Delta u(x_i,y_n)}{|\bar{u}(x_i,y_n)|}, \tag{19}$$

where the error transfer coefficients are

$$K_{ij,m}^{v} = \left| \frac{D_{i,m}^{N_x} \bar{v}(x_m,y_j)}{\sum_{k=0}^{N_x} D_{i,k}^{N_x} \bar{v}(x_k,y_j) - \sum_{k=0}^{N_y} D_{j,k}^{N_y} \bar{u}(x_i,y_k)} \right|, \tag{20}$$

$$K_{ij,n}^{u} = \left| \frac{D_{j,n}^{N_y} \bar{u}(x_i,y_n)}{\sum_{k=0}^{N_x} D_{i,k}^{N_x} \bar{v}(x_k,y_j) - \sum_{k=0}^{N_y} D_{j,k}^{N_y} \bar{u}(x_i,y_k)} \right|. \tag{21}$$

Eq. (19) shows that measurement errors in the velocity data on all the grid points in row i and column j contribute to the error of the computed vorticity at point (x_i,y_j) with the Chebyshev spectral method. In contrast, only the errors on neighboring points contribute to the error of vorticity at that point for low-order schemes such as second-order finite difference and the least-squares method. One implication is that a pure Chebyshev spectral method could be more sensitive to the noise in velocity data than for low-order schemes. For example, it will be shown in Section 4 that for an Oseen vortex at $\delta/R = 0.29$ (R is the dimension of the domain and δ is the characteristic length scale of the Oseen vortex) containing 5% noise, the relative error of vorticity is about 6.1% with the least-squares method, while with the pure Chebyshev spectral method the error is about 17.3%. We will show that the Chebyshev noise processing procedure described in what follows provides a remedy to the noise sensitivity problem of the Chebyshev spectral method.

3.2. Chebyshev noise processing procedure

In general it is not possible to specify the PIV noise distribution in the frequency domain. However, we can expect that the application of the correlation methods for velocity extraction results in a smoothing or low-pass filtering effect, and hence the high-frequency components in the PIV data are usually comprised of noise rather than the physical modes of the flow. These high-frequency noise components significantly affect the calculation of the derivatives and can be detrimental to the success of gradient-based vorticity calculation methods.

We propose the Chebyshev noise processing procedure (CNPP) here, aiming at removing high-frequency noise in PIV experimental velocity data by separating the physical modes (possibly mixed with low-frequency noise modes) from high-frequency noise ones and suppressing the latter in the Chebyshev transform space. This procedure can be applied in conjunction with Chebyshev spectral method.

In CNPP if the number of modes suppressed is too small, we will not remove the majority of high-frequency noise modes. On the other hand, if too many modes are suppressed, some physical modes of the flow could be suppressed as well and we will not achieve the maximum accuracy. Hence, there should be an optimal cut-off mode number, M_{opt}, in CNPP such that when the highest $(N - M_{\mathrm{opt}})$ modes are suppressed, the computed result achieves the minimum error. The optimal mode number can sometimes be determined by examining the Chebyshev coefficient distribution of the data if the distribution demonstrates some kind of "bi-modal" behavior. However, the optimal number of modes to suppress can be difficult to determine in the following situations: (1) When the function does not have a bi-modal spectrum and so we cannot find an obvious separation point between the physical modes and the high-frequency noise modes. (2) The number of grid points is insufficient to resolve the physical structures of the flow such that the physical modes occupy the whole spectrum, and thus suppressing even only the highest mode may affect the flow significantly.

Since the optimal cut-off mode M_{opt} may not always be attainable in reality, we propose a practical procedure

to acquire a quasi-optimal cut-off mode, M_{cut}, based on the energy distribution. Consider a set of one-dimensional experimental data $f(x_j) \pm \Delta f(x_j)$ on Gauss–Lobatto grid points. The energy of the function can be expressed by the inner product

$$(f,f) = \sum_{j=0}^{N} f(x_j) f(x_j) w_j, \tag{22}$$

where $(N+1)$ is the total number of modes and

$$w_j = \begin{cases} \pi/2N, & j = 0, N, \\ \pi/N, & 1 \leqslant j \leqslant N-1. \end{cases} \tag{23}$$

The energy of the measurement error is estimated by,

$$(\Delta f, \Delta f) = \sum_{j=0}^{N} \Delta f(x_j) \Delta f(x_j) w_j. \tag{24}$$

Then we compute the energy ratio

$$\psi_{\text{cut}} = \frac{(\Delta f, \Delta f)}{(f,f)} = \frac{\sum_{j=0}^{N} \Delta f(x_j) \Delta f(x_j) w_j}{\sum_{j=0}^{N} f(x_j) f(x_j) w_j}. \tag{25}$$

The inner product in Eq. (22) can also be expressed in Chebyshev transform space as

$$(f,f) = \sum_{m=0}^{N} \gamma_m f_m f_m, \tag{26}$$

where f_m are the Chebyshev coefficients and

$$\gamma_m = \begin{cases} \pi, & m = 0, N, \\ \pi/2, & 1 \leqslant m \leqslant N. \end{cases} \tag{27}$$

The cut-off mode M_{cut} can then be determined by

$$\sum_{m=M_{\text{cut}}}^{N} \gamma_m f_m f_m = \psi_{\text{cut}} \sum_{n=0}^{N} \gamma_n f_n f_n. \tag{28}$$

To apply CNPP, a mode f_m will be suppressed if $m \geqslant M_{\text{cut}}$. The two-dimensional formulation of this procedure can be obtained in a straightforward way.

4. Result and discussion

The Chebyshev spectral method presented above is evaluated against the least-squares approach [8] first with a simulated Oseen vortex and then with PIV experimental velocity data of the flow past a surface-mounted mixing tab [14].

4.1. Quantitative evaluation with the Oseen vortex

To study the accuracy, noise sensitivity, and the effect of CNPP for the Chebyshev spectral method we take the velocity field of an Oseen vortex and apply both the Chebyshev spectral method and the least-squares method to extract the vorticity field. We can then compare the results against the theoretical result and thus assess the errors of these two methods. The Oseen vortex and its vorticity field in cylindrical coordinates (r, θ, z) can be expressed as

$$v_\theta = \frac{\Gamma}{2\pi\delta} \frac{1}{\eta} (1 - \mathrm{e}^{-\eta^2/4}), \tag{29}$$

$$\omega_z = \frac{\Gamma}{4\pi\delta^2} \mathrm{e}^{-\eta^2/4}, \tag{30}$$

where v_θ is the azimuthal velocity, ω_z is the axial vorticity, Γ is the circulation, $\delta = \sqrt{\nu t}$, and $\eta = r/\delta$. The vortex is placed in the center of a square domain $-R \leqslant x \leqslant R$, $-R \leqslant y \leqslant R$, where R is half the domain width. It is important to note that different values of the parameter δ (vortex core dimension) correspond to different maximum vorticity values of the Oseen vortex. The smaller the parameter δ, the larger the maximum vorticity in the flow. There are 64 grid points in each direction, giving a uniform grid resolution of $0.03R$. Thus in this comparison the parameter δ/R is chosen to vary between 0.03 and 2.0. If we choose $\Gamma = 0.01$ m^2/s and $R = 0.1$ m, the maximum vorticity of the Oseen vortex is varied between 0.02 and 88.9 s^{-1}. The analytic Oseen velocity field is given in both the x and y directions on the Gauss–Lobatto grid points for the Chebyshev spectral method and on uniform grid points for the least-squares method.

As described in [8], in the least-squares method the local velocity field is approximated by a linear combination of a uniform velocity, a line source, a line vortex and a shear layer. Only the line vortex and the shear layer contribute to the out-of-plane vorticity. The decomposition coefficients are determined by a least-squares requirement. When implementing this algorithm, we impose the linear decomposition on all the interior points of the domain. On the boundary points of the domain, however, we use a second-order finite difference method instead since the least-squares method would require grid points that are outside the domain.

Two cases are investigated: (1) velocity fields without noise; (2) velocity fields with noise. For the second case a 5% random noise is superimposed on the analytical Oseen velocity to mimic the noise in experiments in the following manner:

$$u(x,y) = U(x,y) + |U(x,y)| E(x,y) \xi_u(x,y), \tag{31}$$

$$v(x,y) = V(x,y) + |V(x,y)| E(x,y) \xi_v(x,y), \tag{32}$$

where $U(x,y)$ and $V(x,y)$ are the analytic Oseen velocity components, $E(x,y)$ is the amplitude of the noise and chosen as $E(x,y) = E_0 = 5\%$, and $\xi_u(x,y)$ and $\xi_v(x,y)$ are random variables between -1 and 1 generated separately with a random number generator. The same noise field should be used for both the least-squares method and the Chebyshev spectral method. For the Chebyshev spectral method, $\xi_u(x,y)$ and $\xi_v(x,y)$ are generated on the uniform grid first and then interpolated to the Gauss–Lobatto grid points with a bi-quadratic interpolation scheme.

In each case (with and without noise), the vorticity field is computed using both the Chebyshev spectral

method and the least-squares approach. We define the root mean square of the error of computed vorticity,

$$\mathrm{RMS} = \left(\frac{\sum_{i=1}^{N_x-1} \sum_{j=1}^{N_y-1} |\omega_{\mathrm{comp}}(x_i,y_j) - \omega_{\mathrm{ex}}(x_i,y_j)|^2 \cdot A(x_i,y_j)}{\sum_{i=1}^{N_x-1} \sum_{j=1}^{N_y-1} A(x_i,y_j)} \right)^{1/2}, \tag{33}$$

where ω_{comp} is the computed vorticity, ω_{ex} is the exact vorticity, (N_x+1) and (N_y+1) are the number of grid points in x and y directions, and $A(x,y)$ is the area of the grid cell at point (x,y). The global relative error, ε, of vorticity is defined as

$$\varepsilon = \frac{\mathrm{RMS}}{|\omega_{\mathrm{ex}}(0,0)|}, \tag{34}$$

where $\omega_{\mathrm{ex}}(0,0)$ is the exact vorticity at the center of the Oseen vortex. Note that the vorticity data on the outermost layer of grid points are excluded when we compute the error.

At first, the vorticity field of the clean Oseen vortex (without noise) is computed with the Chebyshev spectral method and the least-squares method. The relative error between the computed result and the exact vorticity field is calculated according to Eq. (34) and shown in Fig. 1 with respect to the parameter δ/R. For both methods the relative error ε decreases as δ/R increases in the range of values considered. Clearly, the Chebyshev spectral method is much more accurate than the least-squares method. This superior accuracy is attributed to the fact that, in Chebyshev spectral method, the velocity information on all the points in row i and column j is used to compute the vorticity at point (x_i,y_j).

Next we add 5% random noise to the Oseen vortex velocity field according to Eqs. (31) and (32) and recompute the vorticity field using the Chebyshev spectral method (with and without CNPP) and the least-squares method. We ran the calculations 1024 times each with different seeds for the random number generator. The average relative errors of the computed results are shown in Fig. 2. For all the runs we observe the following trends: with both methods the relative errors increase with respect to δ/R for noisy velocity data. This indicates that the noise affects the vorticity at large δ values (with small velocity gradients) more than at small δ values (with large velocity gradients). With noisy velocity data, the pure Chebyshev spectral method without CNPP consistently gives larger errors than the least-squares method. Hence, we can conclude that the pure Chebyshev spectral method is more sensitive to noise than the least-squares method, which is consistent to our theoretical analysis in Section 3. In order to fully take advantage of the Chebyshev spectral method to calculate velocity derivatives from noisy PIV data it is necessary to perform the Chebyshev noise processing procedure.

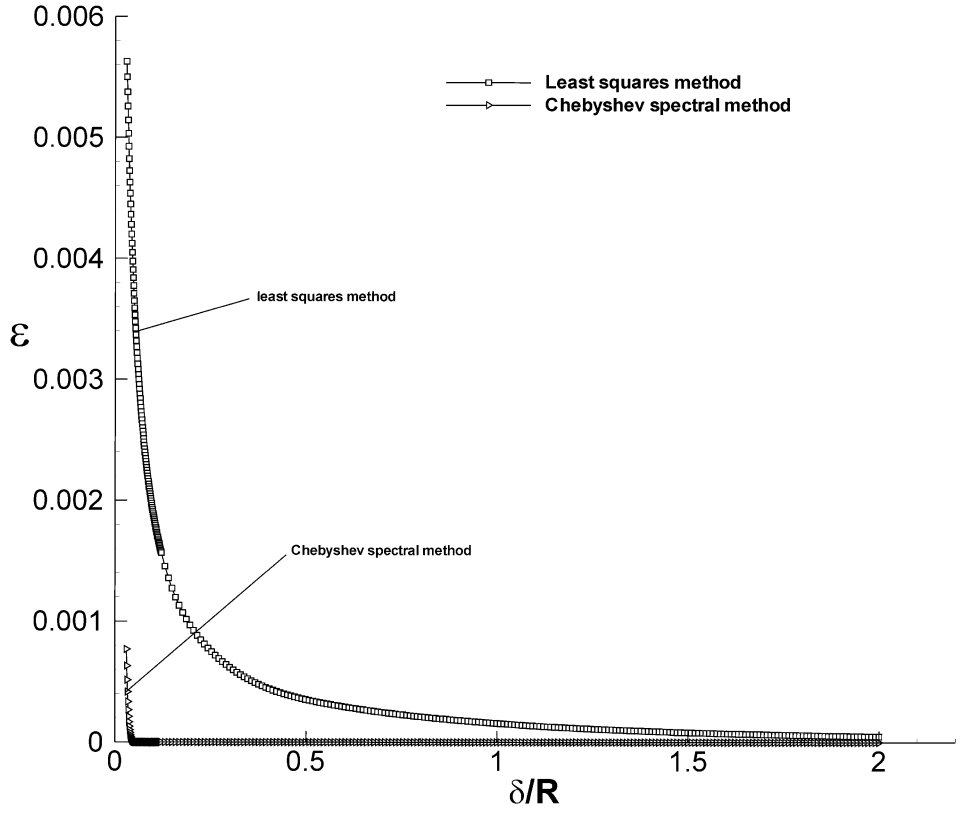

Fig. 1. Dependence of global relative error in vorticity, ϵ, on parameter δ/R for clean Oseen velocity data, 64 grid points in each direction.

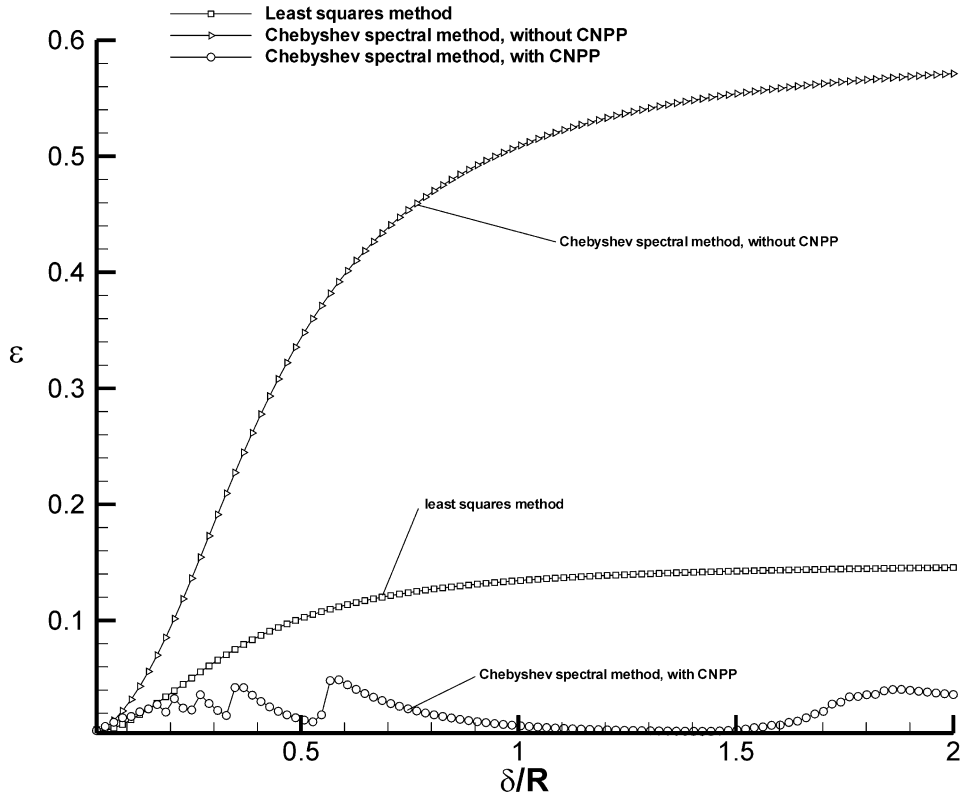

Fig. 2. Dependence of global relative error in vorticity, ϵ, on parameter δ/R for noisy Oseen velocity data, 64 grid points in each direction.

The Chebyshev noise processing procedure introduced in Section 3 can improve the accuracy of the Chebyshev spectral method by removing the high-frequency noise in the data. We next apply the Chebyshev spectral method together with CNPP to re-compute the vorticity of the noisy velocity data. The Chebyshev coefficient $u_{m,n}$ (as well as $v_{m,n}$) is suppressed if

$$((N_x - m)^2 + (N_y - n)^2)^{1/2} < M_{\text{cut}}, \tag{35}$$

where $(N_x + 1)$ and $(N_y + 1)$ are the number of grid points in x and y directions, and M_{cut} is the "cut-off" mode number determined dynamically from Eq. (28). The variation of the relative error ε with respect to the parameter δ/R when CNPP is applied is also shown in Fig. 2. It is evident that CNPP dramatically reduces the error of the vorticity computed using the Chebyshev spectral method, which makes the Chebyshev spectral method more accurate than the least-squares method for almost the entire range of δ values. Fig. 2 shows that the error of the vorticity computed using the Chebyshev spectral method together with CNPP demonstrates stepwise variation with respect to δ/R. The irregularity of the error is caused by the fact that the Chebyshev modes are discrete rather than continuous. As M_{cut} changes with respect to δ/R, the change of the error of vorticity is not smooth. Fig. 3 shows the distributions of the local errors of the vorticity, which are the average of 1024 runs with different seeds fed into the random number generator, along the x axis for different values of δ/R for the noisy Oseen vortex data. For small δ/R values, the error with the least-squares method (Fig. 3(a)) is concentrated at the central region of the vortex. As δ/R increases the gradients of the Oseen vortex spread out and the errors of the vorticity also become distributed in a larger region. For large δ/R values the largest errors of the vorticity are mainly distributed in the region away from the Oseen vortex center with the least-squares method. Similar to the global error in Fig. 2, the local errors of the vorticity using Chebyshev spectral method in conjunction with CNPP also demonstrate stepwise variation with respect to δ/R (Fig. 3(b)). However, compared with those for the least-squares method the local errors are generally smaller. The energy ratio, ψ_{cut}, is estimated for the Oseen vortex as follows. Consider a random relative error E with amplitude E_m ($E_m = 5\%$ for the test Oseen vortex). We assume the relative error to be uniformly distributed on $[-E_m, E_m]$ with a sufficiently large number of data points, so the probability density function (pdf) of the relative error is $\rho(E) = 1/(2E_m)$. Thus the second moment of the relative error or the energy ratio is $\psi_{\text{cut}} = \int_{-E_m}^{E_m} E^2 \rho(E)\,\mathrm{d}E = 1/3E_m^2$. For the test Oseen vortex the energy ratio is$\psi_{\text{cut}} = 1/3 \times 0.05^2 = 8.33 \times 10^{-4}$. Numerical experiments indicate that neither the global nor the local errors of the vorticity change significantly if the estimated energy ratio is larger than 60% of this value and smaller than three times this value. If ψ_{cut} is below 60% of this value the error of the vorticity gradually deteriorates

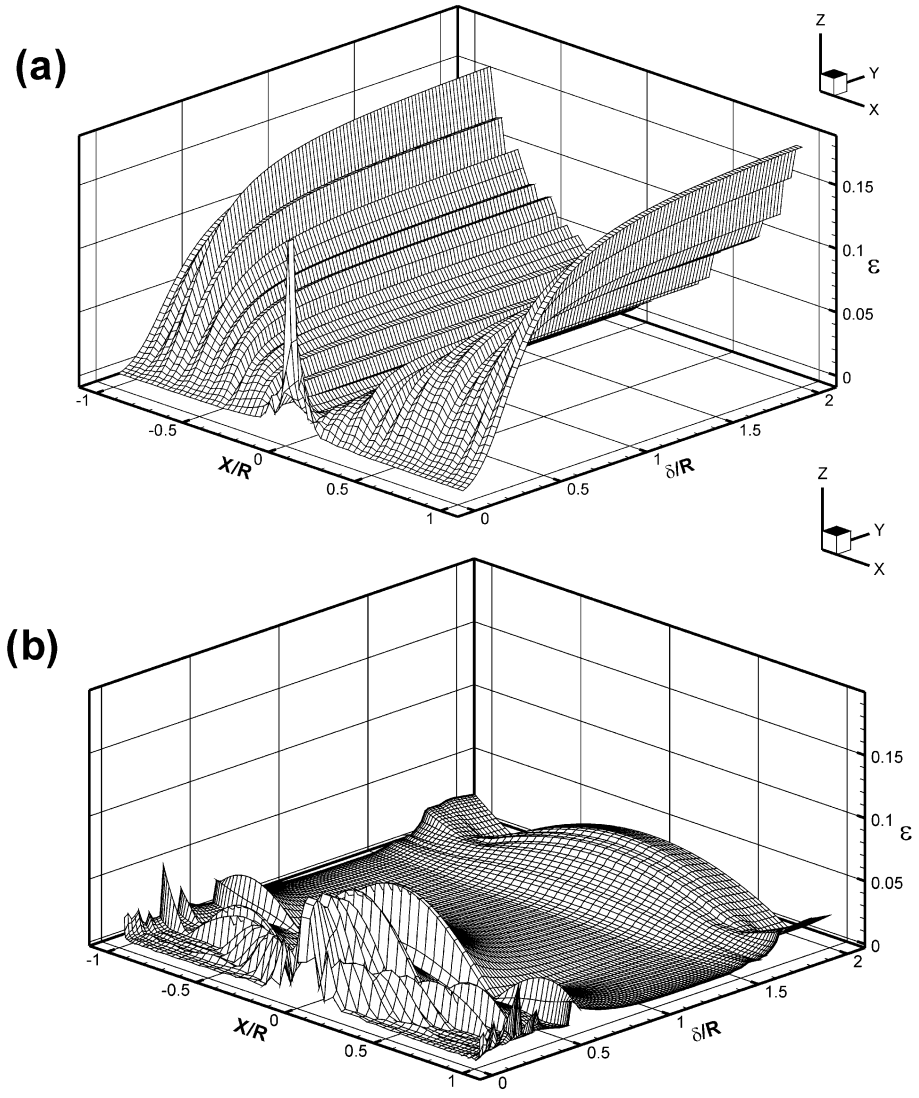

Fig. 3. Local error distribution along the x axis $\varepsilon \sim x/R$ with respect to parameter δ/R of the test Oseen vortex, where $\varepsilon(x) = |\omega_{\text{comp}}(x,0) - \omega_{\text{ex}}(x,0)|/|\omega_{\text{ex}}(0,0)|$. (a) Least-squares method. (b) Chebyshev spectral method with CNPP.

because the unsuppressed high-frequency noise begins to affect the derivatives significantly. If ψ_{cut} is above three times this value the error of the vorticity also deteriorates as the CNPP starts to affect some significant physical modes.

It should be noted that more computations are involved in the Chebyshev spectral method than the least-squares method because all the data points are involved in the calculation of the derivative at any single grid point as shown from the discussion in Section 2. When the CNPP is applied in conjunction with the Chebyshev spectral method even more computation time is needed due to the expensive search to determine the cut-off mode number, M_{cut}, from Eq. (28) in the procedure. In our Oseen vortex tests, on the average the Chebyshev spectral method takes 1.8 times the computation time as the least-squares method. About 10 times the computation time is needed when the CNPP is applied together with the Chebyshev spectral method as compared to the least-squares method.

4.2. Evaluation with PIV data of the wake of a surface-mounted mixing tab

The Chebyshev spectral method and the least-squares method are tested with the PIV experimental velocity data in the center plane of the wake of a surface-mounted mixing tab [14].

The experiments were conducted in a low-speed closed-circuit water tunnel (Fig. 4), with test section of 42.0 cm × 15.5 cm × 18.0 cm (Length × Height × Width). A frequency modulator controls the pump speed, which further controls the free-stream velocity. The uniformity of the flow in the test section is achieved by a combination of flow-straightening device (uniformly stacked straws) and stainless steel wire mesh before the flow

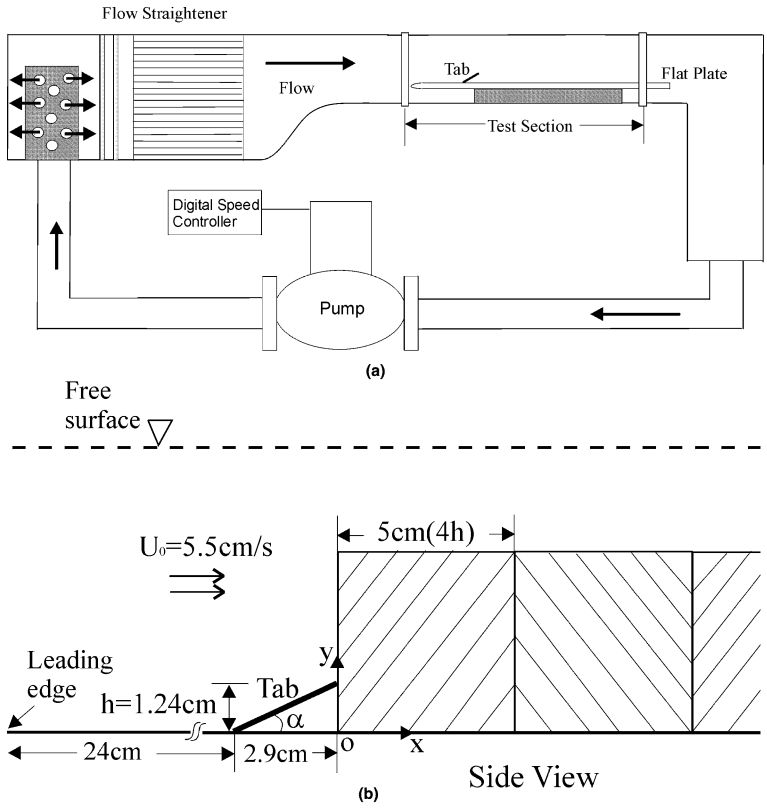

Fig. 4. Experimental setup. (a) Schematic of water tunnel. (b) Measurement window in the center plane of the tab wake.

contracts to the test section. The flow apparatus is documented in detail in Elavarasan and Meng [15]. A symmetric tapered mixing tab is mounted with an inclination angle, $\alpha = 24.5°$, on a smooth horizontal flat plate in the water tunnel 5.5 cm above the bottom wall. The tab is located 24 cm from the elliptical leading edge of the plate. The experiments were carried out at Reynolds number, $Re = U_0 h/v = 600$ based on the free-stream velocity, U_0, and the height of the tab tip above the flat plate (referred to as tab height), h.

The test section is illuminated with a 0.5 mm-thick laser light sheet, which consists of a series of double pulses produced by a pair of digitally sequenced Nd:YAG lasers (Spectra-Physics PIV 400) operating at 10 Hz. The system is filled with distilled water fully seeded with 8–12 um hollow glass particles (TSI 10089) of specific density 1.05–1.15 at a concentration of approximated 50–60 particles/mm^3. PIV images formed by 90° scattering of the seeding particles are recorded by a digital CCD camera (Kodak ES 1.0), and transferred to the host PC via a PCI bus-based frame grabber (Data Translation DT3157). The timing of the double laser pulses and operation of the electric shutter on the CCD camera are synchronized with a digital function generator. Detailed discussions of our PIV system were given in [14,16].

A sliding window is used to select the interrogation cells (IC) of 32×32 pixels for the processing of PIV images. The average displacement for the particles in each IC is calculated using a cross-correlation algorithm with the standard Gaussian-fit sub-pixel technique [17]. After one IC is processed, according to the data point distribution the window is shifted a number of pixels to process the next IC until the whole image is covered.

For the current study the velocity vectors are extracted on two sets of data points: the uniform grid points and the Gauss–Lobatto grid points. To reduce the influence of velocity errors due to the poor PIV image quality on boundaries of the physical region usually caused by illumination inhomogeneities or reflections from solid walls, we extract the velocity vectors on a subdomain of the physical region. We shrink the original region by half an interrogation cell (IC) size on each side and extract velocity in the resulting domain, denoted by $\{(x,y)\,|\,x \in [0,L_1], y \in [0,L_2]\}$. Let (x_{ij}, y_{ij}) denote the center of one typical IC then, for uniform grid points,

$$x_{ij} = \frac{iL_1}{N_x - 1}, \tag{36}$$

$$y_{ij} = \frac{jL_2}{N_y - 1}, \quad i = 0,1,\ldots,N_x - 1,$$

$$j = 0,1,\ldots,N_y - 1 \tag{37}$$

and for the Gauss–Lobatto grid points,

$$x_{ij} = \frac{L_1}{2}\left(1 + \cos\frac{i\pi}{N_x - 1}\right), \tag{38}$$

$$y_{ij} = \frac{L_2}{2}\left(1 + \cos\frac{j\pi}{N_y - 1}\right), \quad i = 0, 1, \ldots, N_x - 1, \quad j = 0, 1, \ldots, N_y - 1, \tag{39}$$

where N_x and N_y are the number of ICs in x and y directions, respectively.

Dynamic mean and median operators [17] are incorporated in our implementation of PIV processing to detect spurious vectors. Missing vectors are filled by the bi-linear interpolation of the four valid neighboring vectors. Still missing data are estimated with the adap-

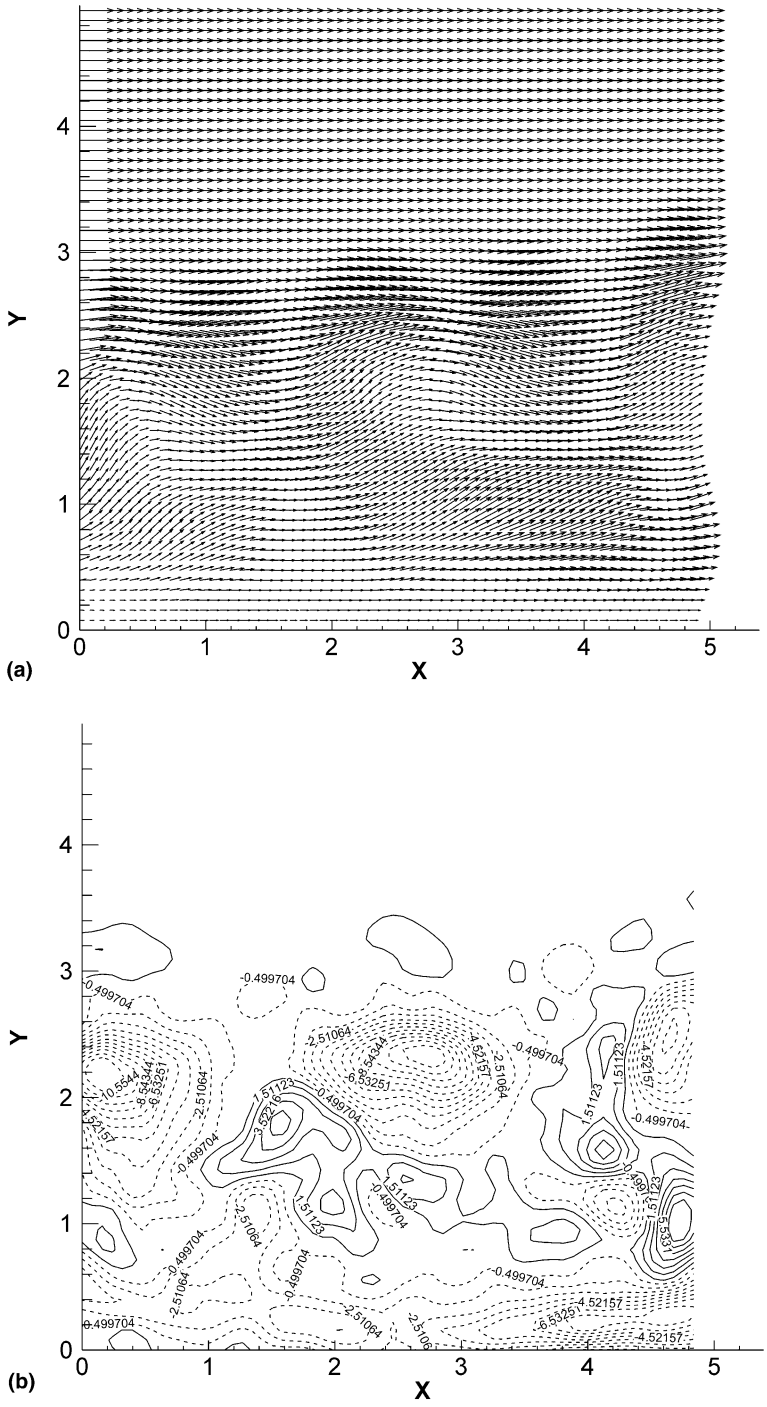

Fig. 5. Instantaneous velocity and vorticity fields in the center plane of flow past a surface-mounted mixing tab, processed on uniformly distributed points, 64 grid points in each direction. (a) Velocity field. (b) Vorticity field of the velocity in Fig. 5(a) computed using the least-squares method.

tive Gaussian window technique [18]. The image and data processing algorithms of our PIV system were documented in detail by [19].

After the velocity vectors of 14 series of PIV realizations (with 20 consecutive realizations in each series) of the tab wake are extracted, the least-squares method is used to compute the vorticity of the velocity data on uniform grid points, and the Chebyshev spectral method together with CNPP is used to compute the vorticity on Gauss–Lobatto grid points. The cut-off mode number is dynamically determined from Eq. (28). The energy ratio ψ_{cut} is estimated in a similar way to that for the test Oseen vortex described in the previous section. For the PIV experiment we choose $E_m = \Delta D/D_{\text{ave}}$, where

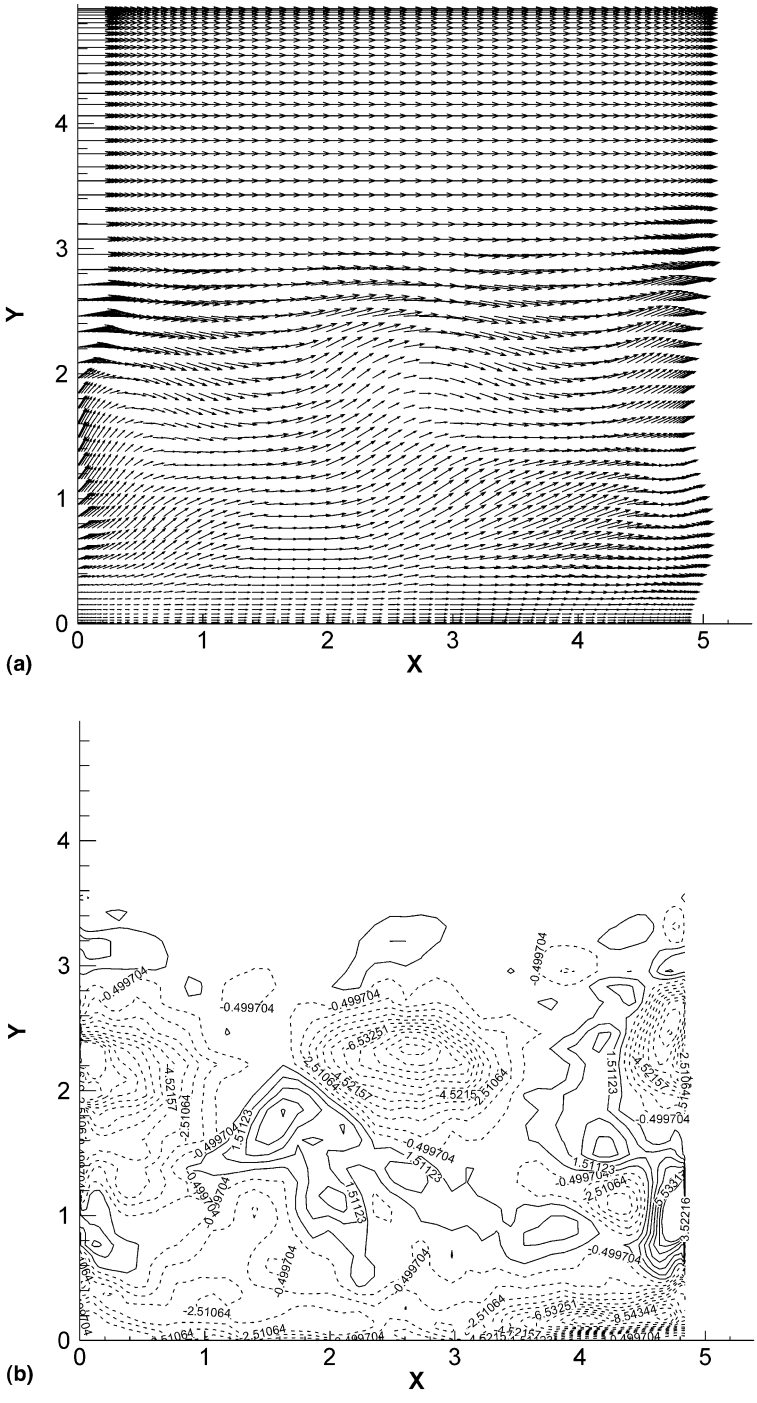

Fig. 6. Instantaneous velocity and vorticity fields in the center plane of flow past a surface-mounted mixing tab, processed on Gauss–Lobatto points, 64 grid points in each direction. (a) Velocity field. (b) Vorticity field of velocity in Fig. 6(a) computed using the Chebyshev spectral method with CNPP.

$$D_{\text{ave}} = \frac{1}{N_x N_y} \sum_{i=0}^{N_x-1} \sum_{j=0}^{N_y-1} |D_{ij}|$$

is the average displacement magnitude of the measured flow field in pixels and the uncertainty of the displacement $\Delta D = 0.5$ because there is still a random uncertainty of 0.5 pixel in the displacement even with subpixel resolution. Figs. 5(a) and 6(a) show the velocity fields of a typical instantaneous PIV realization in the center plane of the tab wake processed on the uniform grid points and the Gauss–Lobatto grid points, respectively. The vorticity fields computed using the least-squares method and the Chebyshev spectral method are shown in Figs. 5(b) and 6(b), respectively. In this example (Fig. 6(a)), $D_{\text{ave}} \approx 6$ and

$$\psi_{\text{cut}} = \frac{1}{3} \times \left(\frac{0.5}{6}\right)^2 = 2.31 \times 10^{-3}.$$

Both methods clearly capture the three vortices passing over the viewing window at $Y = 2$ to 2.5, which have been identified as the cross sections of hairpin vortices [14–16]. Since the "correct" vorticity field of the experimental snapshot is unknown quantitatively, we cannot assess from this example which method gives more accurate vorticity. However, a comparison between the two suggests that both computed vorticity fields are similar qualitatively.

5. Practical significance

The Chebyshev spectral method in conjunction with the Chebyshev noise processing procedure provides a viable alternative way for calculating the vorticity in PIV post-processing to existing methods. Although the Chebyshev spectral method alone is more sensitive to noise than the least-squares method, when used together with the Chebyshev noise processing procedure it is more accurate than the least-squares method in the presence of experimental noise. The Chebyshev noise processing procedure aims at removing high-frequency noise in experimental data by separating the physical modes (possibly mixed with low-frequency noise modes) from the high-frequency noise modes which are detrimental to vorticity calculation and suppressing the latter in the Chebyshev transform space. With appropriate transforms this noise suppression procedure can also be applied in combination with other derivative calculation methods to improve their performance for noisy experimental data.

The Chebyshev spectral method proposed in this paper is restricted to those simplified geometries that can accommodate the special grid requirements. It may not be readily useful for generalized geometries where extensive maskings of the images are required. The Chebyshev spectral method may be particularly relevant to wall-bounded flows because more grid points are located in the region of strongest gradients near the wall. However, it may become unfavorable for free shear flows where the strongest gradients are located in the middle of the domain.

6. Conclusions

The Chebyshev spectral method, together with the Chebyshev noise processing procedure (CNPP), is proposed and investigated for calculating the velocity derivatives of PIV experimental data. The Chebyshev spectral method is very accurate for clean velocity data. However, it is more sensitive to experimental noise than the least-squares method unless it is used in combination with CNPP. In presence of experimental noise the use of the Chebyshev noise processing procedure greatly increases the accuracy of the Chebyshev spectral method by suppressing the high-frequency noise modes in the transform space. The Chebyshev spectral method with CNPP is shown to give higher accuracy than the least-squares method for a wide range of vorticity values. One particular requirement for the application of the method is that the PIV raw images need to be processed on special distributions of data points such as Gauss–Lobatto points.

Acknowledgements

This work was partially supported by the National Science Foundation grant CTS-9625307 and the Kansas Complex Fluid Flow Program when the authors were with Kansas State University. The authors wish to thank J. Sheng for his assistance in the implementation of the PIV image processing on Gauss–Lobatto grid points and W. Yang for the tab flow experimental data. The authors are grateful to X. Song for helpful suggestions on the manuscript. They also wish to thank the anonymous reviewers whose helpful comments contributed to the improvement of the paper.

References

[1] Y. Pu, H. Meng, An advanced off-axis holographic particle image velocimetry (HPIV) system, Exp. Fluids 29 (2000) 184–197.
[2] J. Zhang, B. Tao, J. Katz, Turbulent flow measurement in a square duct with hybrid holographic PIV, Exp. Fluids 23 (1997) 373–381.
[3] D.H. Barnhart, R.J. Adrian, C.D. Meinhart, G.C. Papen, Phase-conjugate holographic system for high-resolution particle image velocimetry, Appl. Opt. 33 (1994) 7159–7169.
[4] J. Jeong, F. Hussain, On the identification of a vortex, J. Fluid Mech. 285 (1995) 69.
[5] J. Soria, B.J. Cantwell, Identification and classification of topological structures in free shear flows, in: J.P. Bonnet, M.N. Glauser (Eds.), Eddy Structure Identification in Free Turbulent Shear Flows, 1993, pp. 379–390.
[6] S.K. Lele, Compact finite difference schemes with spectral-like resolution, J. Comp. Phys. 103 (1992) 16.

[7] K. Mahesh, High order finite difference schemes with good spectral resolution, in: Presented at the Fifth Annual Meeting, American Physical Society/Division of Fluid Mechanics, University of California, Berkeley, San Francisco, 1997.
[8] S. Abrahamson, S. Lonnes, Uncertainty in calculating vorticity from 2D velocity fields using circulation and least-squares approaches, Exp. Fluids 20 (1995) 10.
[9] L. Lourenco, A. Krothapalli, On the accuracy of velocity and vorticity measurements with PIV, Exp. Fluids 18 (1995) 10.
[10] A. Lecuona, J.I. Nogueira, P.A. Rodriguez, Flow field vorticity calculation using PIV data, in: Proceedings of the Second International Workshop on PIV'97-Fukui, Fukui, Japan, 1997.
[11] A. Fouras, J. Soria, Accuracy of out-of-plane vorticity measurements derived from in-plane velocity field data, Exp. Fluids 25 (1998) 409.
[12] C. Cannuto, M.Y. Hussaini, A. Quarteroni, T.A. Zang, Spectral Methods in Fluid Dynamics, Springer, New York, 1988.
[13] M.Y. Hussaini, T.A. Zang, Spectral methods in fluid dynamics, Ann. Rev. Fluid Mech. 19 (1987) 339.
[14] W. Yang, H. Meng, Dynamics of Tab-Wake Vortices, The 52nd Annual Meeting of DFD, American Physical Society, New Orleans, LA, 21–23 November 1999.
[15] R. Elavarasan, H. Meng, Flow visualization study of role of coherent structures in a tab wake, Fluid Dynamics Res. 27 (2000) 183.
[16] W. Yang, H. Meng, J. Sheng, Hairpin vortices generated by a mixing tab in a channel flow, Exp. Fluids, (2001), in press.
[17] M. Raffel, C. Willert, J. Kompenhans, Particle Image Velocimetry, Springer, Berlin, 1998.
[18] J.C. Agui, J. Jimenez, On the performance of particle tracking, J. Fluid Mech. 185 (1987) 447.
[19] J. Sheng, Development of data processing systems, algorithms, and application for PIV and Holographic PIV, M.S. thesis, Mechanical Engineering, Kansas State University, 1998.